How can pH drop while adding NaOH? Formation and transformation of Mn4(OH)6SO4

Damien Cornu, Romain Coustel, Pierrick Durand, Cédric Carteret, Christian Ruby

How can pH drop while adding NaOH? Formation and transformation of $Mn_4(OH)_6SO_4$

Damien Cornu,*,† Romain Coustel,† Pierrick Durand,‡ Cédric Carteret,† and Christian Ruby*,†

†*LCPME UMR 7564, Université de Lorraine - CNRS, F-54000 Villers-lès-Nancy, France*

‡*CRM2 UMR 7036, Université de Lorraine, CNRS, F-54000 Vandoeuvre-lès-Nancy, France*

E-mail: damien.cornu@univ-lorraine.fr; christian.ruby@univ-lorraine.fr

Abstract

It is expected that during a titration using a basic NaOH solution, the pH can only increase. In this article the formation of two different solids during the precipitation of a $MnSO_4$ solution is discussed. The formation of a new compound $Mn_4(OH)_6SO_4 \cdot nH_2O$ instead of $Mn(OH)_2$ is evidenced by the quantification of the remaining ions in solution as well as by X-Ray Diffraction, Raman and infrared spectroscopies. The transformation of this solid into $Mn(OH)_2$ after a sursaturation of the solid in OH^- can explain a drop of the pH in the titration curve.

Introduction

The product expected through the basification of a Mn^{2+} solution is $Mn(OH)_2$[1,2] even if some salt incorporating sulfate and hydroxide anions are observed experimentally through the basicification of solutions prepared from $MnSO_4 \cdot H_2O$ salt, as mentioned by Zhao *et al.*[3] and Zhang *et al.*[4] This solid is $Mn_9(OH)_{14}(SO_4)_2 \cdot H_2O$ but is never observed alone,

often associated with pyrochroite $Mn(OH)_2$ and more oxidised form of manganese (Mn_3O_4). With hydrothermal treatment, it is possible to produce other salt combining manganese, hydroxide and sulfate, like $Mn_3(OH)_2(SO_4)_2 \cdot (H_2O)_2$ [5] and $Mn_2(OH)_2SO_4$.[6] $Mn_5(OH)_8SO_4$ that were produced by slow precipitation using cyclohexyl amine. These basic salts are cited for applications such as pulp bleaching.[3,4]

Table 1: Manganese sulfate basic salts salts

R	Salt formula	Ref
0.75	$Mn_3(OH)_2(SO_4)_2 \cdot (H_2O)_2$	[5]
0.75	$Mn_3(OH)_2(SO_4)_2 \cdot (H_2O)_2 \cdot K_2SO_4$	[7]
1	$Mn_2(OH)_2SO_4$	[6]
1.5	$Mn_4(OH)_6(SO_4)$	*This work*
1.55	$Mn_9(OH)_{14}(SO_4)_2 \cdot H_2O$	[3,4]
1.6	$Mn_5(OH)_8SO_4$	[8]

According to Pattanayak and coworkers,[9] the oxidation products of solids obtained through the basicification of a $MnSO_4$ solution is Mn_3O_4 if the pH of the solution is 9 whereas the solid obtained at pH = 13 is oxidised into Mn_2O_3. It is possible that the solid obtained at pH = 9 is not the same as the one obtained at pH =13. The influence of the quantity of base on the precipitation is studied using two different basic salts, $MnCl_2$ or $MnSO_4$. Both were precipitated using a NaOH. It appears that a new solid, with the formula $Mn_4(OH)_6SO_4 \cdot nH_2O$ is obtained from the sulfate manganese salt until the addition of 1.5 OH^- molecule per Mn^{2+} cation. XRD, Raman and IR studies indicate that this solid is different from $Mn(OH)_2$ or other known manganese sulfate basic salts.

This solid could be used for environmental purposes, such as denitrification, hydrogen peroxide decomposition but also to better understand the oxidation of Mn^{2+} in natural waters.[2]

The precipitation of this solid is associated with a peculiar acid-base titration curve with pH as a function of the quantity of OH^- added. These curves can have various shapes, depending on the strength, concentration of the acidic molecules as well as the multiplicity of protons that can be released by each molecule. For an homogeneous solution, it should be

shaped like a sigmoid with inflexions points expected at the equivalence points. Precipitation adds some complexity to the curves, because it adds a new constraint as long as the solid exists.[10]

It is expected that during a titration using a basic NaOH solution, the pH can only increase. However, a small drop of the pH during metallic ions titration with NaOH is reported as the consequence of a sursaturation of the solution prior to the precipitation.[10] Here, the precipitation of $Mn_4(OH)_6SO_4 \cdot nH_2O$ and its transformation into $Mn(OH)_2$ triggers a drop in the pH curves as the quantity of aqueous OH^- ions reacting with the basic salt is larger than the quantity added at each step from the burette.

Results and discussion

50 mL of a 0.4 mol.L^{-1} $MnCl_2$ or $MnSO_4$ solution are poured in the isotherm titration flask of an automated titrator at 18°C. Initial pH is 5.5, as expected, because Mn^{2+} is surrounded by 18 water molecules, creating a cluster with a pKa equals to 10.6.[11]

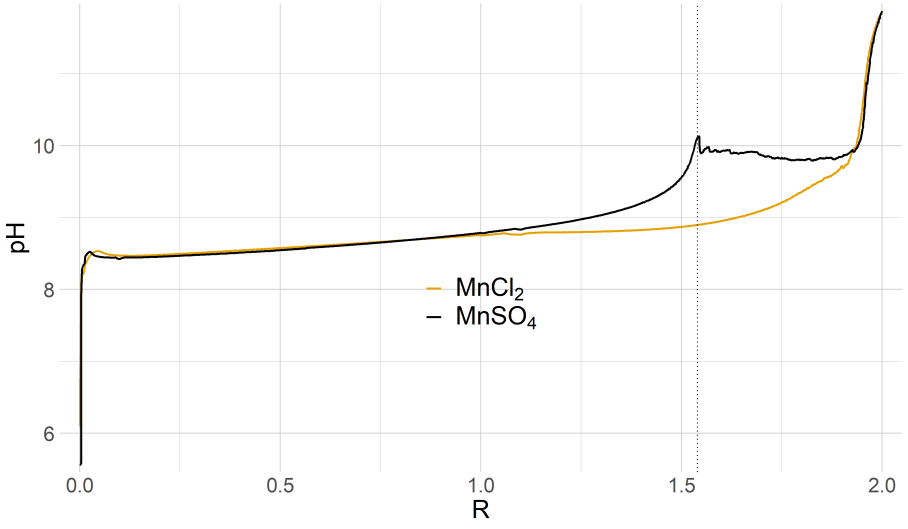

Figure 1: Titration curve of $MnCl_2$ and $MnSO_4$ solutions as a function of R = $\frac{n(OH^-)}{n(Mn^{2+})}$

The titration curves for two different Mn salts are shown on Figure 1. pH is plotted as a function of $R = \frac{n(OH^-)}{n(Mn^{2+})}$ indicating the amount of hydroxide ion added in the solution

compared to the initial amount of manganese.

The solutions with $MnCl_2$ follows a classical basic precipitation curve. During the addition of sodium hydroxide over the manganese solutions, a white solid precipitates. The apparition of a precipitate is linked with an angular point as it is related to a new constraint driving the variation of the pH, the precipitation plateau.[10] The solubility constant $K_S = [Mn^{2+}][OH^-]^2$ is calculated to be 4 x 10^{-12}± 1 x 10^{-12} using the pH value and the expected concentration for various R. This is larger than the reported one at 18°C ($9x10^{-13}$)[12] as the precipitation occurs in a solution containing chloride ions and not in pure water.[13] A very small pH local maximum is observed very close to R = 0, reaching a value of 8.53 and decreasing after until reaching 8.47. This local maximum was already observed for the precipitation of $Zn(OH)_2$, and explained by Eggermont *et al.*: to initiate precipitation, stable nuclei need to form and this requires an amount greater than the theoretical amount of OH^- needed to initiate precipitation. A quick addition of NaOH creates a small heterogeneity in the concentration allowing this precipitation, but with a completely homogeneous solution, the precipitation can be avoided until an excess of NaOH exist in the whole solution. This phenomenon can be compared to the supercooling of liquid.[14] According to X-Ray Diffraction, this solid is $Mn(OH)_2$ for all R values in agreement with the literature,[15] the co-precipitation with Cl is only achieved under harsh temperature and pression conditions.[16] A final increase of the pH is observed for R = 1.96 as the quantity of aqueous manganese in the solution decreases. The small difference with the theoretical R = 2 value for $Mn(OH)_2$ is perhaps linked with the fact that, even with nitrogen bubbling, a small proportion of manganese is oxidised (see figure S2 and associated text). Interestingly a similar titration curve is obtained for $Mn(NO_3)_2$ solution as well as for $MnCl_2$ solution (results not shown).

The titration curve for $MnSO_4$ solution is different. First, the precipitation occurs for slightly lower pH (8.42) and therefore a smaller sursaturation. But the main difference is a very reproducible experimental cusp for R = 1.53 and pH = 10.13. This cusp is unchanged with bigger or smaller increments or with a slower or quicker addition of the NaOH solution,

as long as the addition increment is lower than 0.05 mL (a larger addition leads to brutal changes for the stability of the pH for R values above 1.5). The cusp is not a simple kinetic artefact: if the titration is stopped at R = 1.5, the pH is stable during hours as long as the solution is kept under nitrogen bubbling.

To understand this titration curve, we analysed the remaining quantities of aqueous cations and anions in solution for the the $MnSO_4$ salt. Quantities are indicated on Figure 2 and were measured with Inductively Coupled Plasma (aqueous Mn species) and ionic chromatography (SO_4^{2-}). Solid line show the theoretical quantities in solution for the production of pyrochroite $Mn(OH)_2$ (eq 1). If the precipitate is $Mn(OH)_2$, the quantity of sulfate in solution should not be affected.

$$Mn^{2+}(aq) + 2OH^-(aq) \longrightarrow Mn(OH)_2(s) \quad (1)$$

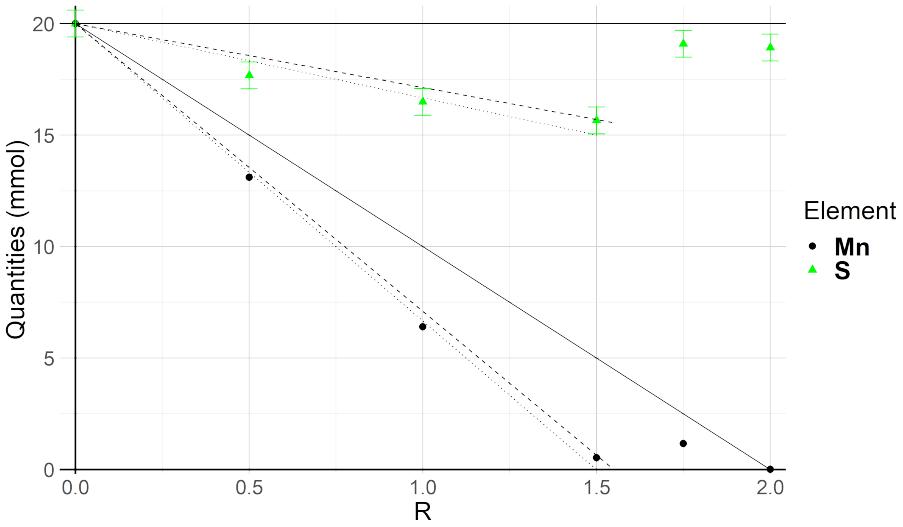

Figure 2: Soluble Mn (black circles) and SO_4^{2-} (green triangles), from ICP-MS measurement and ionic chromatography respectively, for a $MnSO_4$ solution as a function of the R ratio. Error bars for Mn are smaller than the mark (0.1 mmol). Solid lines for the quantitative formation of $Mn(OH)_2$, dotted lines for the formation of $Mn_4(OH)_6SO_4$, and dashed lines for the one of $Mn_9(OH)_{14}(SO_4)_2 \cdot H_2O$

Dotted lines show the theoretical quantities in solution if a basic salt with the composition $Mn_9(OH)_{14}(SO_4)_2 \cdot H_2O$ precipitates, dotted line for the one of $Mn_4(OH)_6SO_4$ (eq 2). One

should note that the proposed composition omits any additional water molecules inserted in the structure of this basic salt (*i.e.* the formula should have been written $Mn_4(OH)_6(SO_4) \cdot n(H_2O)$ with n the number of water molecules associated with the salt).

$$4Mn^{2+}(aq) + {SO_4}^{2-}(aq) + 6OH^-(aq) \longrightarrow Mn_4(OH)_6(SO_4)(s) \quad (2)$$

Results shown in Figure 2 suggest that the latter solid is produced. The formation of several different salts leading together to the precipitation of similar amounts of Mn and ${SO_4}^{2-}$ ratio cannot be excluded. Nevertheless, the solid obtained for R = 1.5 shows close EDS spectra when taking spectra 2 μm apart from each others, then the solid appears homogeneous at this scale.

This solid, obtained at R = 1.5, was not described previously in the literature. Its R ratio is however close to the $Mn_9(OH)_{14}(SO_4)_2 \cdot H_2O$ ratio (1.55) described by Zhang[4] and Zhao[3] (see table 1).

From the pH values (Figure 1) and the concentrations (Figure 2), the solubility constant K_S of the $Mn_4(OH)_6(SO_4)$ solid was determined in the order of magnitude of 10^{-36}.

X-ray diffraction of the solids with various R values obtained from $MnSO_4$ solution were shown on Figure 3. In agreement with the literature, for R = 2, a single pyrochroite $Mn(OH)_2$ phase is obtained. For R = 1.5, the diffractogram is more complex, and broad peaks of pyrochroite with a small intensity appear along shaper peaks. There is no match for the later with the ICDD database. The structure is in agreement with a trigonal or hexagonal lattice and with the following parameters: a = 8.7227 Å and c = 14.8686 Å. Tables S1 and S2 show the attribution of the XRD peaks in those structures. It is interesting to note that the volume of the hexagonal or trigonal cell of the new structure is close to half of the one of $Mn_9(OH)_{14}(SO_4)_2 \cdot H_2O$ (rhombohedral) with a = 8.626 Å and c = 29.200 Å.

The characterization of the solid is always performed on the wet sample. Drying the R = 1.5 sample under nitrogen flow leads to a different diffractogram (SI Figure S3) with some remaining peaks of the previously described structure as well as peaks of $Mn_9(OH)_{14}(SO_4)_2 \cdot H_2O$

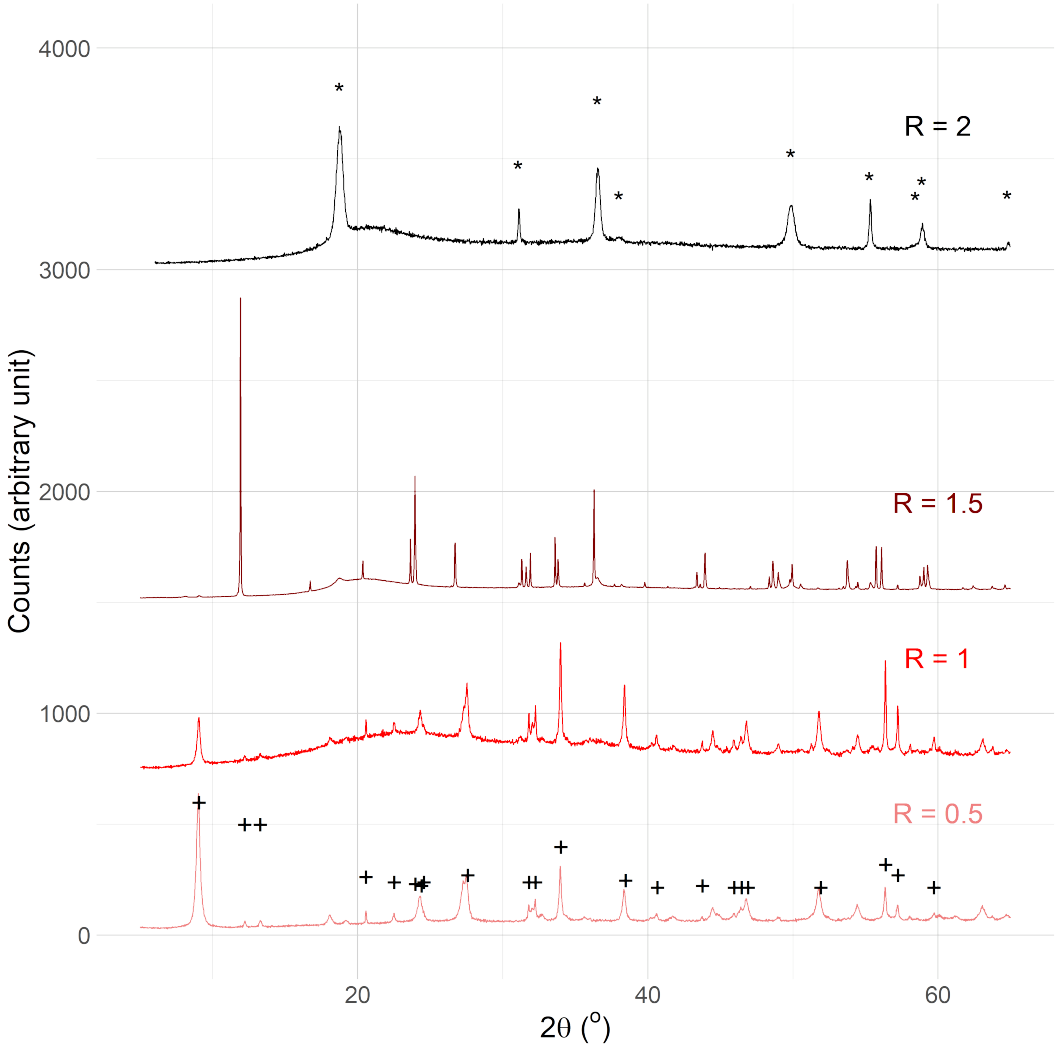

Figure 3: XRD patterns of the wet solids obtained from $MnSO_4$ solution after the addition of OH^- for R from 0.5 to 2. Stars depict the position and intensities reported for pyrochroite $Mn(OH)_2$ (JCPDS 01-073-1604), Cross depict the position and intensities reported for $Mn_9(OH)_{14}(SO_4)_2 \cdot H_2O$ (JCPDS file 00-018-0788). Samples were covered with glycerol which explains the bump around $2\theta = 20°$

(JCPDS file 00-018-0788) and some of the remaining Na_2SO_4 solid. As the solid is stable only in wet environment, one cannot therefore determine the number of water molecules within the molecular formula without a complete description of the structure, for instance with Rietveld refinement of the XRD data. This characterization is out of scope of this article. The proximity of the chemical compositions of $Mn_4(OH)_6(SO_4)$ and $Mn_9(OH)_{14}(SO_4)_2 \cdot H_2O$ can be helpful for this task. Indeed, the cristallographic cell of $Mn_9(OH)_{14}(SO_4)_2 \cdot H_2O$ is close to two cells of $Mn_4(OH)_6(SO_4)$ joined together.For lower R values, the diffractograms show that a solid containing $Mn_9(OH)_{14}(SO_4)_2 \cdot H_2O$ is produced.

In addition to the measurements on figure 2, a confirmation of the transformation in the solid for R above 1.5 is the infrared measurements (FTIR) of the damp solids through attenuated total reflexion (ATR) after centrifugation. SI Figures S4 and S5 show that in addition of the O-H stretching (3300 cm^{-1}) and H_2O bending (1636 cm^{-1}) modes, the R = 1.5 sample absorbs the IR light at 1080 and 1119 cm^{-1}, which is typical for the sulfate ions.[17] This is not the case for the solid obtained at R = 2. This result indicates that sulfate ions are eliminated.

Another confirmation arise form the Raman spectra obtained for solid with R between 0.5 and 2 (SI Figure S6). The two emission peaks at low frequencies (529 and 459 cm^{-1}) observed for the three solids R = 0.5, 1 and 1.5, shift to lower wavenumbers (504 and 406 cm^{-1}) for the solid obtained at R =2. Few studies report Raman spectra of pyrochroite as this material is easily transformed into Mn_3O_4 under laser radiation. However, it has a brucite-like structure with a Mn-OH A_{1g} vibration Raman active at 401 cm^{-1} according to Lutz and coworkers.[18] Unfortunately, their study does not look at the vibrations above 450 cm^{-1}. However, the typical brucite structure has three main peaks, one with a E_g symmetry and two with a A_{1g} symmetry, the 504 cm^{-1} could be the E_g peak as expected for this kind of structure.[18] Beside, concerning the vibration attributed to the sulfate anion, the intensity of the ν_1 vibration (around 1000 cm^{-1}) of the sulfate anion on the R = 2 sample is much lower than for R = 0.5, 1 and 1.5. The remaining 983 cm^{-1} vibration is typical for the Na_2SO_4

compound.[19] The wet sample dries during the Raman experiment which can explain the presence of this solid. This indicates that, as seen in IR, the sulfate ions are not inserted within the structure of the solid.

The formula of the solid obtained for R = 1.5 is $Mn_4(OH)_6SO_4 \cdot nH_2O$. pH at this point is above 10, which is quite over the pH observed for the titration of the $MnCl_2$ solution (see Figure 1). This is because the quantity of Mn remaining in solution is very low ($6.5x10^{-6}$ $mol.L^{-1}$ according to ICP measurement) and therefore, for the same solubility constant, the OH^- concentration has to rise up. At that point, XRD shows some badly cristallized $Mn(OH)_2$ particles. As the pH increase, the stability of this $Mn(OH)_2$ particle over the basic sulfate manganese salt increases. The formation of $Mn(OH)_2$ triggers a drastic pH change when R is higher than 1.5. Indeed, according to equation 3, an aqueous Mn release is evidenced at R = 1.75 by ICP-MS. The metallic cation reacts then quickly with the hydroxide ions according to equation 1 leading to the decrease of the pH observed during the titration. Reactions 3 and 1 consume more hydroxide than the amount added from the burette, leading to the drop in the pH.

$$Mn_4(OH)_6(SO_4)(s) \longrightarrow 3Mn(OH)_2(s) + Mn^{2+}(aq) + {SO_4}^{2-}(aq) \tag{3}$$

The overall reaction 4 has an equilibrium constant equal to 4.10^9 as calculated from the constants for reaction 1 and 3, which mean that a pH higher than 8.9 is needed to trigger the reaction. This may explain why this transformation does not occur for low R values. As for the nucleation, a sursaturation of the solution in OH^- can be necessary to initiate this transformation.

$$Mn_4(OH)_6(SO_4)(s) + 2\,HO^-(aq) \rightleftharpoons 4Mn(OH)_2(s) + {SO_4}^{2-}(aq) \tag{4}$$

Conclusion

The precipitation of a novel Mn basic salt with the formula $Mn_4(OH)_6SO_4 \cdot nH_2O$ is evidenced by quantification of the remaining ions in the solution as well as with XRD, Raman and IR spectroscopy. Upon drying, this solid is partially transformed into $Mn_9(OH)_{14}(SO_4)_2 \cdot H_2O$. During the titration of $MnSO_4$ solution, the synthesis of this solid requires less hydroxides ions than the pyrochroite $Mn(OH)_2$, which leads to a sursaturation of the solution in OH^- up to a ratio R = $n(OH^-)/n(Mn^{2+})$ about 1.5. Then, upon NaOH addition, $Mn_4(OH)_6SO_4$ is transformed into $Mn(OH)_2$, capturing more hydroxide ions than the one added by the burette, leading to a drop of the pH. This explain how we can get a drop of the pH while adding NaOH.

Experimental section

Titration

The titration was performed with a 50 mL of a $MnSO_4 \cdot H_2O$ (Sigma Aldrich, $\geq$99%) solution (0.4 mol.L^{-1}) in a refrigerated flask at 18°C with a variable volume of a 1 mol.L^{-1} NaOH (VWR 31627.290) to reach the desired R value ($R = \frac{n(OH^-)}{n(Mn^{2+})}$) under stiring and nitrogen bubling. The NaOH solution is added with very small steps (0.01 mL) and a waiting time allowing the stabilisation (drift smaller than 20 mV/min or at least 10 s). The pH was registered with a Metrohm pH electrode Unitrode with Pt1000 and a Toledo Inlab redox electrode.

Characterization

Characterization of the solid was performed on fresh wet solid shortly after preparation.

ICP-MS

Released manganese concentrations in the solution were measured by Inductively Coupled Plasma Mass Spectroscopy (ICP-MS Agilent-7800). 100 μL of the supernatant solution after centrifugation was diluted in 100 mL with water. The calibration curve in the range 50 to 2000 ppb has been established from Sigma-Aldrich 74128 samples. The detected isotopes was ^{55}Mn.

Ionic chromatography

Sulfate concentration was determined by ion chromatography. Analysis were performed with a Metrohm 882 Compact IC plus instrument equipped with chemical (Metrohm suppressor MSM II) and sequential (Metrohm CO2 suppressor MCS) suppressors and a conductimetric detector. The eluent (1.8 mmol.L^{-1} Na_2CO_3 and 1.7 mmol.L^{-1} $NaHCO_3$ solution) flowed continuously through a Metrosep A Supp 4 - 250/4.0 column associated with a guard column (Metrosep A supp 4/5 guard). Standards solutions were prepared from a commercial 1000 μg.mL^{-1} anions (Merck 1.11448.0500). The flow rate and the injected volume were respectively 1 mL.min^{-1} and 20 μL.

XRD

The products were measured soon after the synthesis and the centrifugation. XRD diffractograms were recorded either on wet or dried samples. For wet samples, excess of water was removed by pressing the water soaked paste between tissues. The resulting paste was measured on an approximately 10 μm thick zero background X-ray holder covered with a minimal amount of glycerol to protect the paste from air oxidation, as the compounds were known to be air sensitive. The x^2 Multiple (at least 15) 1h X-ray scans were collected, and the diffractograms did not show any sign of evolution, the multiple scans were summed up for better X-ray statistics.

Powder X-ray diffraction patterns were recorded with a Panalytical X'Pert Pro MPD

diffractometer in reflection geometry using a tube with Cu radiation ($K\alpha_1$ = 1.5406 Å), a Ge(111) incident-beam monochromator, 0.02 rad Soller slits, programmable divergence and antiscatter slits (the irradiated area was fixed to 10 mm x 10 mm), and an X'Celerator detector. Data were collected from finely ground samples with a sample holder spinner and continuous rotation of sample to improve statistical representation of the sample.

Vibrational spectroscopies

- *Infrared* IR measurements of the wet solids were recorded under nitrogen flow in a Attenuated Total Reflectance mode on a Bruker Tensor 27 spectrometer equipped with a KBr beam splitter and a deuterated triglycine sulfate (DTGS) thermal detector. Spectra were recorded and processed using OPUS 7.5 software (Bruker, Karlsruhe, Germany).

- *Raman* 10 μL sample were collected, centrifugated and the wet sample were deposited over a aluminium plate and inserted into the spectrometer. Then Raman spectra were collected on a Renishaw inVia™Qontor ®microspectrometer equipped with a confocal microscope and an Olympus X50 objective (N.A = 0.55). A 532 nm exciting radiation was used with a laser power below 0.05 mW for all samples to prevent their degradation. The spot area was of few μm^2. Several locations were probed on each sample. The spectral resolution was about 4 cm^{-1} and the precision on the wavenumber was lower than 1 cm^{-1}.

Acknowledgement

We thank the spectroscopy and microscopy Service Facility of SMI LCPME (Université de Lorraine-CNRS http://www.lcpme.cnrs-nancy.fr). In addition, we thank Claire Genois and Christelle Despas for the ICP-MS analysis and the ionic chromatography. We would also like to thank the plateforme PMD^{2}X de l'Institut Jean Barriol de l'Université de Lorraine.

Supporting Information Available

Supplementary information are available on *This page*. All the raw data and the R codes used to generate them using the Tidyverse packages[20] are available on `https://github.com/dacornu/Mn-salt-data/`.

References

(1) Moore, T. E.; Ellis, M.; Selwood, P. W. Solid Oxides and Hydroxides of Manganese1. *Journal of the American Chemical Society* **1950**, *72*, 856–866, Publisher: American Chemical Society.

(2) Morgan, J. J. Kinetics of reaction between O2 and Mn(II) species in aqueous solutions. *Geochimica et Cosmochimica Acta* **2005**, *69*, 35–48.

(3) Zhao, H.; Wu, H.; Hu, H.; Li, Y.; Li, J.; Zhang, X. Cooperative Decomposition of Hydrogen Peroxide by Lignin-combined Transition Metals in Pulp Bleaching. *BioResources* **2018**, *13*, 3922–3931.

(4) Zhang, X.; Li, Y.; Wang, L.; Sha, L.; Hu, Z. Investigation of manganese hydrolysis particles and decomposition of hydrogen peroxide in the pulp bleaching process. *Nordic Pulp & Paper Research Journal* **2015**, *30*, 578–583.

(5) Salah, M. B.; Vilminot, S.; André, G.; Richard-Plouet, M.; Bourée-Vigneron, F.; Mhiri, T.; Kurmoo, M. Synthesis, Nuclear, and Magnetic Structures and Magnetic Properties of [Mn3(OH)2(SO4)2(H2O)2]. *Chemistry – A European Journal* **2004**, *10*, 2048–2057.

(6) Salah, M. B.; Vilminot, S.; Mhiri, T.; Kurmoo, M. Synthesis, Crystal Structure, and Magnetic Properties of Mn2(OH)2SO4: A Novel Layered Hydroxide. *European Journal of Inorganic Chemistry* **2004**, *2004*, 2272–2276.

(7) Yu, J.-H.; Ye, L.; Ding, H.; Chen, Y.; Hou, Q.; Zhang, X.; Xu, J.-Q. Structural characterization of a layered double salt Mn3(OH)2(SO4)2(H2O)2·K2SO4. *Inorganic Chemistry Communications* **2007**, *10*, 159–162.

(8) Fan, Y.; Li, G. H.; Yang, L.; Zhang, Z. M.; Chen, Y.; Song, T. Y.; Feng, S. H. Synthesis, Crystal Structure, and Magnetic Properties of a Three-Dimensional Hydroxide Sulfate: Mn5(OH)8SO4. *European Journal of Inorganic Chemistry* **2005**, *2005*, 3359–3364.

(9) Pattanayak, J.; Rao, V. S.; Maiti, H. S. Preparation and thermal stability of manganese oxides obtained by precipitation from aqueous manganese sulphate solution. *Thermochimica Acta* **1989**, *153*, 193–204.

(10) Eggermont, S. G. F.; Prato, R.; Dominguez-Benetton, X.; Fransaer, J. Metal removal from aqueous solutions: insights from modeling precipitation titration curves. *Journal of Environmental Chemical Engineering* **2020**, *8*, 103596.

(11) Li, J.; Fisher, C. L.; Chen, J. L.; Bashford, D.; Noodleman, L. Calculation of Redox Potentials and pKa Values of Hydrated Transition Metal Cations by a Combined Density Functional and Continuum Dielectric Theory. *Inorganic Chemistry* **1996**, *35*, 4694–4702, Publisher: American Chemical Society.

(12) CRC Handbook of Chemistry and Physics, 87th ed Editor-in-Chief: David R. Lide (National Institute of Standards and Technology). CRC Press/Taylor and Francis Group: Boca Raton, FL. 2006. 2608 pp. $139.95. ISBN 0-8493-0487-3. *Journal of the American Chemical Society* **2007**, *129*, 724–724.

(13) Willey, J. D. The Effect of Ionic Strength on the Solubility of an Electrolyte. 2004; `https://pubs.acs.org/doi/pdf/10.1021/ed081p1644`, Archive Location: world Publisher: Division of Chemical Education.

(14) Moore, E. B.; Molinero, V. Structural transformation in supercooled water controls the

crystallization rate of ice. *Nature* **2011**, *479*, 506–508, Number: 7374 Publisher: Nature Publishing Group.

(15) Um, N.; Hirato, T. Precipitation behavior of Ca(OH)2, Mg(OH)2, and Mn(OH)2 from CaCl2, MgCl2, and MnCl2 in NaOH-H2O solutions and study of lithium recovery from seawater via two-stage precipitation process. *Hydrometallurgy* **2014**, *146*, 142–148.

(16) Falkowski, V.; Zeugner, A.; Isaeva, A.; Ruck, M.; Huppertz, H. Synthesis and Characterization of the New Manganese Hydroxide Chloride -Mn(OH)Cl. *European Journal of Inorganic Chemistry* **2018**, *2018*, 4630–4637.

(17) Lane, M. D. Mid-infrared emission spectroscopy of sulfate and sulfate-bearing minerals. *American Mineralogist* **2007**, *92*, 1–18.

(18) Lutz, H. D.; Möller, H.; Schmidt, M. Lattice vibration spectra. Part LXXXII. Brucite-type hydroxides M(OH)2 (M = Ca, Mn, Co, Fe, Cd) — IR and Raman spectra, neutron diffraction of Fe(OH)2. *Journal of Molecular Structure* **1994**, *328*, 121–132.

(19) Mabrouk, K. B.; Kauffmann, T. H.; Aroui, H.; Fontana, M. D. Raman study of cation effect on sulfate vibration modes in solid state and in aqueous solutions. *Journal of Raman Spectroscopy* **2013**, *44*, 1603–1608, _eprint: https://onlinelibrary.wiley.com/doi/pdf/10.1002/jrs.4374.

(20) Wickham, H. et al. Welcome to the Tidyverse. *Journal of Open Source Software* **2019**, *4*, 1686.

Graphical TOC Entry